



# Delineation of supergene enrichment, hypogene and oxidation zones utilizing staged factor analysis and fractal modeling in Takht-e-Gonbad porphyry deposit, SE Iran



Peyman Afzal<sup>a,b</sup>, Mohammad Eskandarnejad Tehrani<sup>a,c,\*</sup>, Majid Ghaderi<sup>d</sup>, Mohammad Reza Hosseini<sup>d</sup>

<sup>a</sup> Department of Mining Engineering, Faculty of Engineering, South Tehran Branch, Islamic Azad University, Tehran, Iran

<sup>b</sup> Camborne School of Mines, University of Exeter, Penryn, UK

<sup>c</sup> Young Researchers and Elite Club, South Tehran Branch, Islamic Azad University, Tehran, Iran

<sup>d</sup> Department of Economic Geology, Tarbiat Modares University, Tehran, Iran

## ARTICLE INFO

### Article history:

Received 13 July 2015

Revised 27 November 2015

Accepted 4 December 2015

Available online 9 December 2015

### Keywords:

Staged factor analysis (SFA)

Concentration–volume (C–V) fractal modeling

Takht-e-Gonbad porphyry Cu deposit

Logratio matrix

## ABSTRACT

The aim of this study is to delineate the different mineralized zones consisting of supergene enrichment hypogene and oxidation zones in Takht-e-Gonbad porphyry Cu deposit (SE Iran), subsurface data and using the staged factor analysis (SFA) and concentration–volume (C–V) fractal modeling. Results obtained by SFA reveal that Cu and Mo were situated in a factor as F1–5 which was modeled by C–V fractal modeling for separation of the mineralized zones. The supergene enrichment zone obtained by the SFA and C–V fractal modeling contains 1.16% for Cu and 241 ppm for Mo. Moreover, the hypogene zone derived via the SFA and C–V fractal modeling has Cu and Mo mean values of 0.65% and 109 ppm. These mineralized zones were correlated with geological models utilizing logratio matrix which indicate that the obtained zones based on the SFA and C–V fractal model are consistent with the geological models. The results derived via logratio matrix reveal overlapping between geological and mathematical models. As a result, combination of the C–V fractal modeling and SFA can be used to delineate mineralized zones based on multivariate data.

© 2015 Elsevier B.V. All rights reserved.

## 1. Introduction

Since 1904, porphyry copper deposits have represented the main resource/reserve of copper all around the world. This type of deposits is the most important with respect to high tonnage of ore values for Cu, Mo, Au and Sn. One of the essential studies on the porphyry deposits is identifying mineralized zones particularly supergene enrichment and hypogene zones (Robb, 2005; Berger et al., 2008; Pirajno, 2009). Conventional geological methods for detection and recognition of supergene enrichment and hypogene zones in the porphyry deposits are based on mineralogical and petrographical studies (e.g., Lowell and Guilbert, 1970; Cox and Singer, 1986; Berger et al., 2008). However, statistical analysis and mathematical methods have been utilized to distinguish mineralized zones since the 1950s (e.g., David, 1970; Davis, 2002). The main aim of statistical analysis, particularly factor analysis, is to extract a few ‘factors’ to raise the ability of illustrating multivariate data (Treiblmaier and Filzmoser, 2010; Yousefi et al., 2012, 2014). Staged factor analysis is one of multivariate statistical techniques which can reduce variables (elements) and define paragenetic elements in different factors (Yousefi et al., 2014).

Fractal/multifractal modeling has been widely used in the mineral exploration and economic geology specifically for the identification of geochemical anomalies and mineralized zones (e.g., Cheng et al., 1994; Agterberg, 1995; Li et al., 2003; Zuo et al., 2009; Afzal et al., 2011; Hassanpour and Afzal, 2013; Rahmati et al., 2014). Several fractal models have been developed and proposed in geochemical exploration to separate geochemical populations, e.g., concentration–area (C–A: Cheng et al., 1994), concentration–distance (C–D: Li et al., 2003), number–size (N–S: Mandelbrot, 1983) and its 3D form by Sadeghi et al. (2012), simulated size–number (SS–N: Sadeghi et al., 2015) and concentration–volume (C–V: Afzal et al., 2011) based on surface and subsurface data. In this paper, the staged factor analysis is used for reducing factor and defining paragenesis factor for Cu and Mo and utilized the C–V multifractal model for separating various mineralized zones in Takht-e-Gonbad porphyry deposit, SE Iran, and the results are correlated with the geological modeling.

## 2. Methodology

### 2.1. Staged factor analysis

Multivariate statistical methods such as factor analysis supposes that data have normal (symmetric) distribution; however, geochemical exploration data never demonstrate a normal distribution (Reimann and

\* Corresponding author at: Department of Mining Engineering, Faculty of Engineering, South Tehran Branch, Islamic Azad University, Tehran, Iran.

E-mail address: [mohammad.eskandarnejad@gmail.com](mailto:mohammad.eskandarnejad@gmail.com) (M.E. Tehrani).

Filzmoser, 2000; Yousefi et al., 2012; Yousefi and Carranza, 2015a). The major purpose of the factor analysis is to realize a few and common factors from multivariate data (Treiblmaier and Filzmoser, 2010; Yousefi et al., 2012; Yousefi and Carranza, 2015b). The accuracy of the factor value measurements changes with element concentration; these values are less accurate at very low and high concentrations (Reimann and Filzmoser, 2000). The geochemical data distribution are not symmetric and most of geochemical data are compositional data (Filzmoser et al., 2009; Yousefi et al., 2012; Yousefi and Carranza, 2015c) which means that they system in which individual variable are not independent of each other (Carranza, 2011). Therefore, normalization operation must be applied to these data. In this paper, the natural logarithm (Ln) was used for transforming values of multivariate geochemical data in a classical factor analysis by SPSS v. 23 software. After transformation of geochemical data, standard techniques such as classical estimation of correlation matrix were used to find the relation between all the variables. More over principal component analysis (PCA) is utilized to extract principal components for identifying hidden multivariate data structures and decreasing the number of variables (Filzmoser et al., 2009; Yousefi et al., 2012; Gholami et al., 2012). The staged factor analysis consists of two main phases as follows:

The first phase is for extraction of 'clean' factors and the second phase is for extraction of a significant multi-element zonation signature of the mineral deposit-type sought to calculate reliable loadings and factor scores. On the other hand, elements are not situated in any factors should be rejected for generating clean factors. Each of the main phases of the staged factor analysis may comprise sub-phases depending on geochemical data and the mineral deposit-type sought (Yousefi et al., 2014).

In this paper, five stages of factor analysis were carried out to achieve main multi-element anomalous geochemical data of Takht-e-Gonbad deposit. These elements are Cu, Mo and Ag and the final stage was named F1–5. This Stage was used in the C–V fractal modeling for identifying zones.

## 2.2. Concentration–volume (C–V) fractal modeling

Afzal et al. (2011) proposed the C–V fractal model for delineation of mineralized zones and barren host rocks in different ore deposits, especially in porphyry Cu deposits, this model can be expressed as:

$$V(\rho \leq v) \propto \rho^{-a1}; V(\rho > v) \propto \rho^{-a2} \quad (1)$$

where  $V(\rho \leq v)$  and  $V(\rho > v)$  indicate volumes (V) with concentration values ( $\rho$ ) smaller and greater than contour values ( $v$ ), respectively,  $a1$  and  $a2$  are characteristic exponents.

Different mineralized zones in the ore deposits (Cu porphyry deposit in this scenario) have fractal properties and are defined by power law relationships between their ore element concentrations and volumetric extensions. Represented breakpoints in C–V log–log plots of concentration values versus volumes separate geochemical populations by threshold values. Breakpoints in the log–log plots outlined various populations of geochemical concentration values representing different lithological and mineralogical zonation.

## 3. Geological setting of the study area

### 3.1. Regional geology

The Takht-e-Gonbad porphyry Cu deposit is situated about 70 km NE of the Sirjan city, SE Iran. Most of the Cu porphyry deposits of Iran occurred in the Cenozoic Urumieh–Dokhtar magmatic belt which is one of the subdivisions of the Zagros orogenies (Alavi, 1994; Dargahi et al., 2010; Asadi et al., 2014). These are particularly revealed in the SE arc segment which is referred to Kerman Cenozoic magmatic arc (KCMA) with 450 km length and 60–80 km width (Fig. 1: Shafiei et al., 2009; Asadi et al., 2014). The KCMA is situated on the western

boundary of the Central Iranian block with calc-alkaline intrusive rocks (stocks) association (Asadi et al., 2014).

The Takht-e-Gonbad deposit is located on the center and south of KCMA as (Fig. 1). The initial exploration was started in the 1970s by Yugoslavian geologists and the result was impregnation tuffs as host rocks (Geological Survey of Iran, 1973). Based on the geological map of Takht-e-Gonbad deposit, Eocene volcanic–pyroclastic rocks and Neogene sediments such as carbonate units are the main rocks in the deposit (Fig. 1). Phyllic, argillic, propylitic, silicic and carbonate alteration zones were resulted in the Miocene granodiorite intrude to Eocene volcanic–pyroclastic rocks. Phyllic alteration is the main alteration type and is accompanied by hypogene zone in the Takht-e-Gonbad deposit. The region surrounding the deposit is tectonically active and most of the faults occurring in this deposit are affected by Nain–Baft fault (Hosseini, 2012; Fig. 1).

### 3.2. Mineralization and alteration

Mineralization in the KCMA occurred in quartz stockworks, veins and as spread sulfides in both the host stock and surrounding the older volcanic and pyroclastic rocks (e.g., Shafiei et al., 2009; Asadi et al., 2014). At Takht-e-Gonbad deposit, oxide, hypogene and immature supergene zones have been developed. The supergene enriched zone is distinguished mainly by chalcocite and covellite. This zone varies in thickness from 10 to 50 m (Hosseini et al., 2011; Hosseini, 2012).

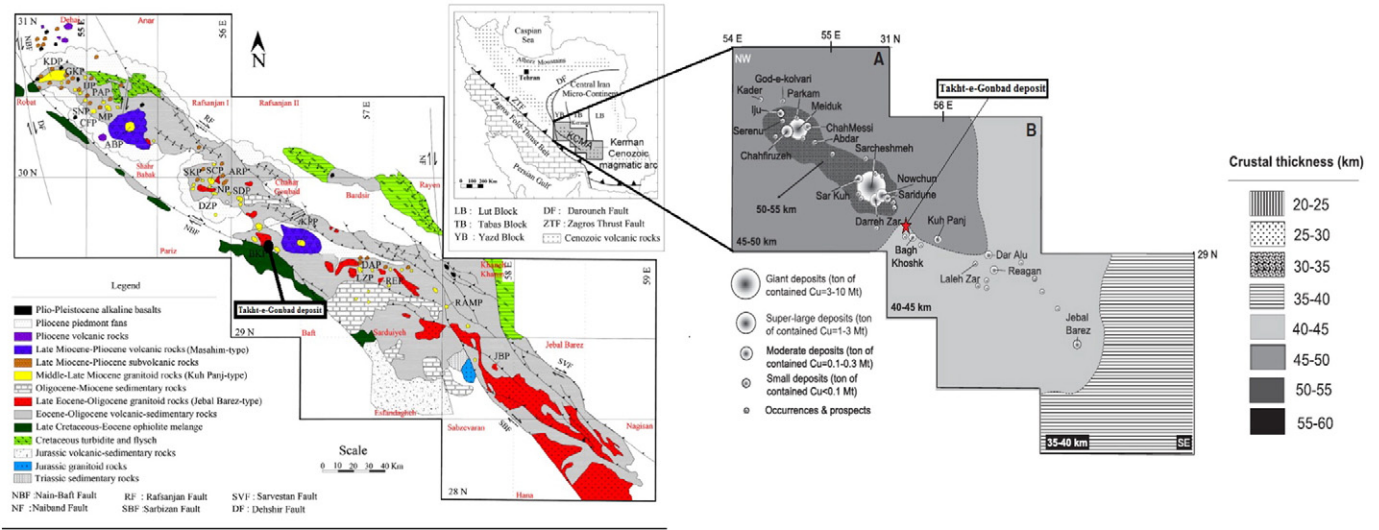
Hypogene ore at Takht-e-Gonbad consists of pyrite, chalcopyrite and minor magnetite and molybdenite. The hypogene ore of economic grade has been traced for about 150 m below the oxide ore (Hosseini, 2012; Table 1). One of the important features of the deposit area is the N–S fracturing system which appears as late barren dykes and breccia pipes (Taghipour et al., 2008; Hosseini et al., 2011; Asadi et al., 2014). Hydrothermal alteration at Takht-e-Gonbad was distinguished by an extensive phyllic assemblage and irregular zones of propylitic and calc-silicate assemblages. Copper mineralization in the deposit is associated mainly with phyllic alteration zone. Maximum Cu grade is higher than 5%, however, it is rare, based on the logging and analysis of the drill cores.

## 4. Discussion

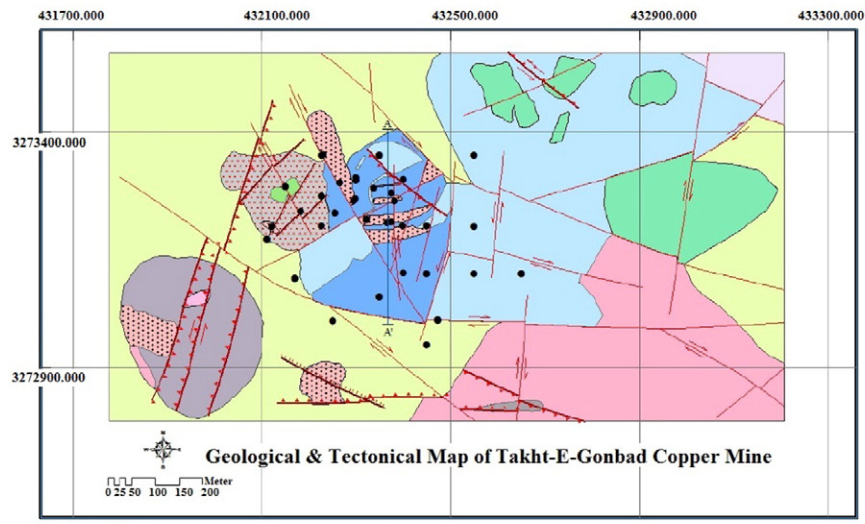
In this study, 39 drilled boreholes data including collar coordinates, azimuth, orientation (dip), lithology, alteration and mineralogy were used to create the 3D geological modeling, and also, the zonation, alteration, lithology and mineralization models were generated by RockWorks™ v.15 software package (Fig. 2). Based on the geological modeling, phyllic alteration zone, the granodiorite rocks and hypogene zone are expanded in the area and chalcopyrite is the major ore element in the deposit. From the drilled boreholes, 2830 litho-geochemical samples were collected and analyzed by ICP-AES for Cu, Mo, Ag, Cd, Co, Cr, Fe, Mo, Ni, Sb, Mn and Zn. Distribution of Cu and Mo were not normal. Therefore, natural logarithm transformer was applied to transform data distribution to symmetric the F1–5 in the geostatistical and fractal modeling. The experimental semi-variogram for F1–5 data in the Takht-e-Gonbad deposit is demonstrate a range, nugget effect and spatial variance of 81 m, 0.418 and 0.536 %, respectively built up by Datamine Studio software (Fig. 3).

### 4.1. Application of staged factor analysis

In factor analysis, a threshold value for minimum loading criterion for elemental variables should be selected between the ranges of 0.3 to 0.6 in order to reduce the errors of the calculation of the scores (Fabrigar et al., 1999; Davis, 2002; Filzmoser et al., 2009). Consequently, the absolute value of 0.5 will be a medium loading value (Treiblmaier and Filzmoser, 2010; Yousefi et al., 2012, 2014). In this study, 0.6 was selected for the minimum loading criterion. The classical principal factor



(a)



(b)

**Fig. 1.** a) Cenozoic Urumieh–Dokhtar magmatic belt of Iran and distribution size of Iranian porphyry Cu deposits and landscapes with Moho depth and crustal thickness (km) in the KCMA (Asadi et al., 2014). b) Geological map of Takht-e-Gonbad deposit (Hosseini, 2012).

analysis for extracting the common factors was applied within varimax method (Kaiser, 1958). This method used for rotated factors with eigenvalues more than 1 for interpretation, utilized staged factor analysis and achieved stages to extract clean factor (common and more existing elements) of the Takht-e-Gonbad deposit (Table 2). In the first stage

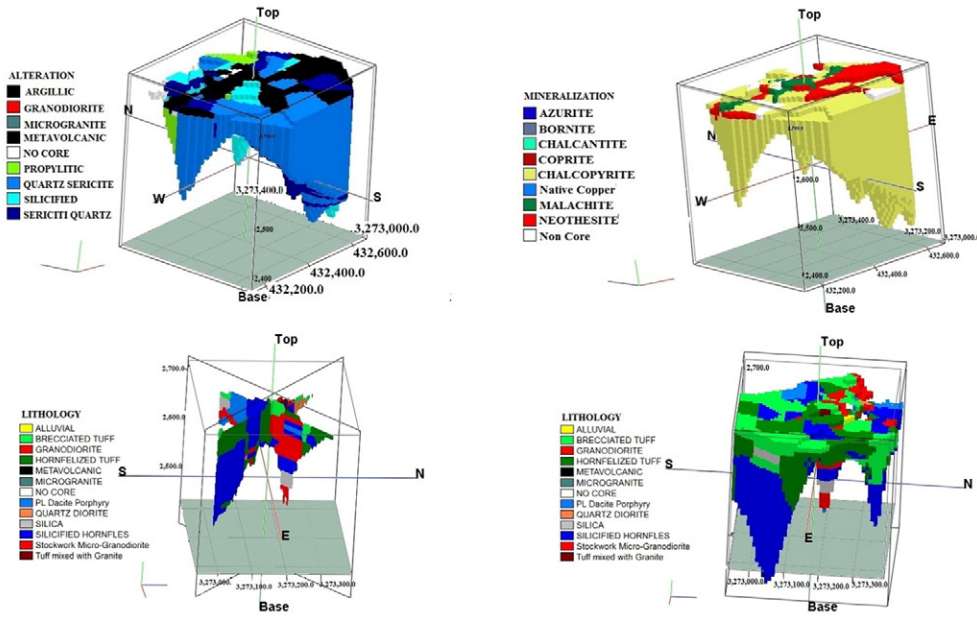
**Table 1**  
Petrographical, mineralogical and alteration particulars of the Takht-e-Gonbad porphyry deposit.

Rock types	Ore minerals	Alteration
Major: Granodiorite	Major: Chalcopyrite	Phyllic (major) Calc-silicate
Minor: Quartz monzonite Tonalite	Minor: Bornite, Pyrite	Propylitic Argillic (supergene)

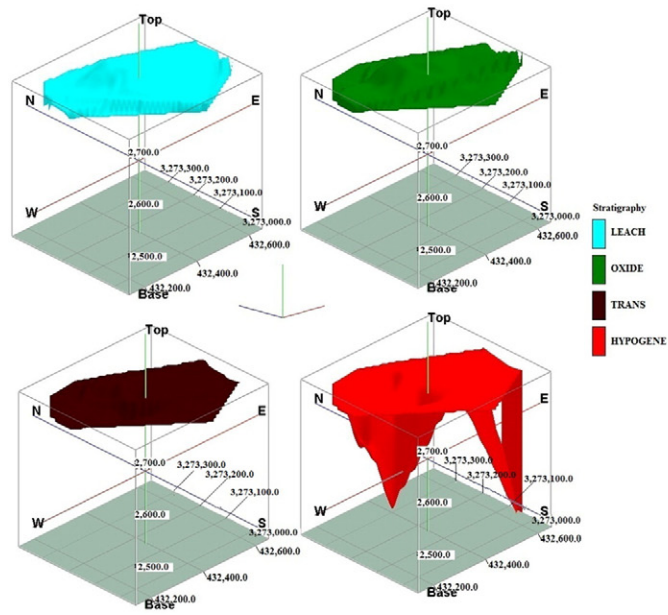
of factor analysis, several elements are not in contact with any factor with due attention to select threshold value for loading were excluded from the data set which are noise elements or geochemical noise that are not in any groups (factors). After excluding noise elements, the second stage of factor analysis was executed on the remaining data to build new factors. If there are some elements not associated with any factors, those are excluded from the data set. Additionally, third stage was executed because all noise elements were rejected and clean factor were generated (Yousefi et al., 2014).

In the first stage of factor analysis, five factors were separated (Table 2). Factor 2 represents Ag, Cu and Mo association which is the main factor based on the main ore elements. After five stages of factor analysis, factor 5–1 is the clean factor and perform in component matrix because only one component was extracted and the solution could not be rotated. The other factors were rotated and shown in rotated

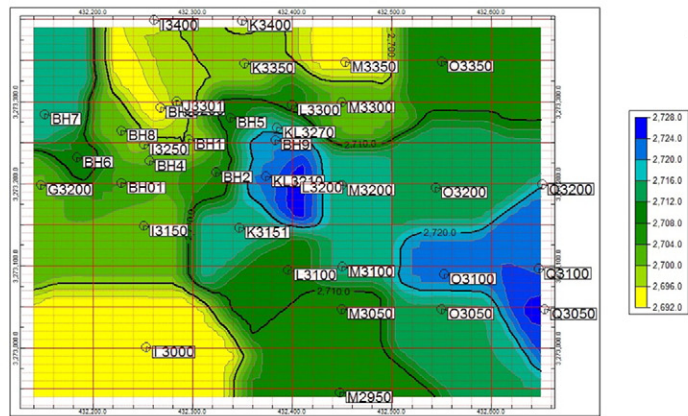




(a)



(b)



(c)

Fig. 2. a) Alteration, mineralization, lithology and fence lithology 3D models, b) zonation models and c) borehole location of Takht-e-Gonbad deposit.

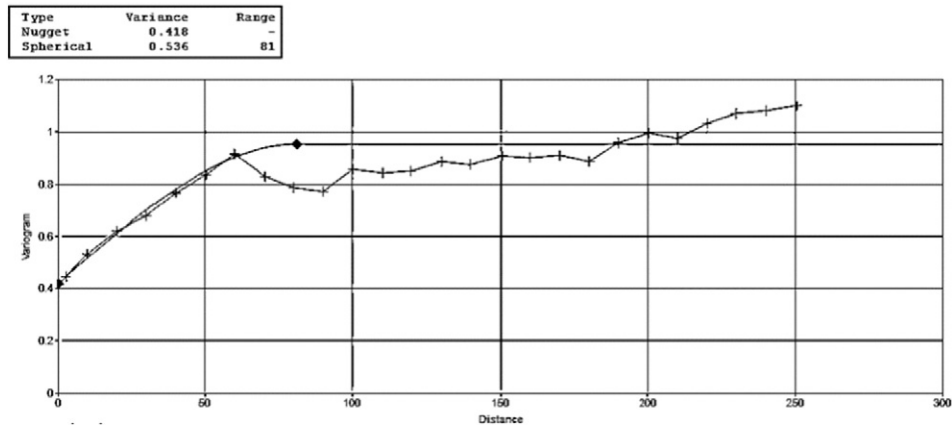


Fig. 3. The experimental semi-variogram for F1–5 data in the studied deposit.

Table 2  
Rotated factor matrix for five stages of staged factor analysis.

Rotated Component Matrix

	First Stage					
	1	2	3	4	5	6
Ln Ag	0.181	<b>0.709*</b>	0.121	0.167	-0.033	0.359
Ln As	0.402	0.131	0.099	<b>0.720</b>	0.124	0.124
Ln Ca	-0.115	-0.108	0.113	-0.095	<b>0.857</b>	0.056
Ln Cd	-0.123	0.077	-0.027	0.139	0.260	<b>0.776</b>
Ln Co	<b>0.859</b>	0.092	0.105	0.072	0.076	0.145
Ln Cr	-0.058	-0.007	<b>0.942</b>	-0.140	0.016	-0.005
Ln Cu	0.316	<b>0.764</b>	0.001	-0.036	-0.353	0.047
Ln Fe	<b>0.918</b>	0.080	0.000	0.026	-0.069	0.095
Ln Mn	0.486	-0.090	0.092	0.260	<b>0.690</b>	0.018
Ln Mo	-0.111	<b>0.809</b>	-0.120	-0.074	0.056	-0.037
Ln Ni	0.170	-0.033	<b>0.919</b>	0.087	0.164	-0.018
Ln P	<b>-0.303</b>	<b>0.380</b>	<b>0.208</b>	<b>-0.576</b>	<b>0.349</b>	<b>0.080</b>
Ln Pb	0.430	-0.013	-0.079	0.056	-0.069	<b>0.733</b>
Ln Sb	-0.041	0.152	0.149	<b>0.626</b>	0.288	0.285
Ln V	<b>0.230</b>	<b>0.168</b>	<b>0.322</b>	<b>-0.698</b>	<b>0.219</b>	<b>0.071</b>
Ln Zn	0.394	0.342	0.125	-0.052	-0.246	<b>0.601</b>

Extraction Method: PCA, Rotation Method: Varimax with Kaiser Normalization, Rotation converged in 7 iterations

\*Bold Values: above threshold value

Rotated Component Matrix

	Second Stage				
	1	2	3	4	5
Ln Ag	0.218	<b>0.745*</b>	0.092	0.245	0.207
Ln As	0.372	0.076	0.005	<b>0.772</b>	-0.012
Ln Ca	<b>-0.192</b>	<b>-0.357</b>	<b>0.319</b>	<b>0.143</b>	<b>0.586</b>
Ln Cd	0.042	0.194	-0.092	0.206	<b>0.747</b>
Ln Co	<b>0.848</b>	0.042	0.146	0.194	-0.009
Ln Cr	-0.050	0.069	<b>0.935</b>	-0.098	0.002
Ln Cu	0.310	<b>0.803</b>	-0.014	-0.024	-0.209
Ln Fe	<b>0.867</b>	0.059	-0.024	0.216	-0.184
Ln Mn	<b>0.373</b>	<b>-0.331</b>	<b>0.247</b>	<b>0.468</b>	<b>0.327</b>
Ln Mo	-0.179	<b>0.705</b>	-0.033	0.021	0.054
Ln Ni	0.152	-0.035	<b>0.923</b>	0.169	0.006
Ln Pb	<b>0.648</b>	0.176	-0.115	-0.067	0.527
Ln Sb	-0.051	0.110	0.019	<b>0.799</b>	0.221
Ln Zn	<b>0.571</b>	<b>0.528</b>	<b>0.050</b>	<b>-0.074</b>	<b>0.263</b>

Extraction Method: PCA, Rotation Method: Varimax with Kaiser Normalization, Rotation converged in 8 iterations

\*Bold Values: above threshold value

Rotated Component Matrix

	Third Stage			
	1	2	3	4
Ln Ag	0.251	<b>0.732*</b>	0.094	0.339
Ln As	<b>0.519</b>	<b>-0.004</b>	<b>0.075</b>	<b>0.539</b>
Ln Cd	-0.007	0.128	-0.067	<b>0.748</b>
Ln Co	<b>0.892</b>	0.097	0.144	0.026
Ln Cr	-0.082	0.035	<b>0.945</b>	-0.040
Ln Cu	0.325	<b>0.828</b>	-0.017	-0.127
Ln Fe	<b>0.909</b>	0.064	-0.005	-0.031
Ln Mo	-0.171	<b>0.801</b>	-0.066	0.022
Ln Ni	0.151	-0.053	<b>0.942</b>	0.093
Ln Pb	<b>0.559</b>	<b>0.138</b>	<b>-0.115</b>	<b>0.350</b>
Ln Sb	0.077	-0.040	0.102	<b>0.791</b>

Extraction Method: PCA, Rotation Method: Varimax with Kaiser Normalization, Rotation converged in 5 iterations

\*Bold Values: above threshold value

Rotated Component Matrix

	Fourth and Fifth Stages			
	1	2	3	4
Ln Ag**	0.240	<b>0.734*</b>	0.091	0.353
Ln Cd	-0.029	0.113	-0.047	0.783
Ln Co	0.907	0.102	0.127	0.078
Ln Cr	-0.068	0.026	0.954	-0.042
Ln Cu	0.317	<b>0.839</b>	-0.028	-0.128
Ln Fe	0.934	0.075	-0.033	0.017
Ln Mo	-0.188	<b>0.799</b>	-0.060	0.014
Ln Ni	0.165	-0.051	0.938	0.085
Ln Sb	0.099	-0.037	0.080	0.809

Extraction Method: PCA, Rotation Method: Varimax with Kaiser Normalization, Rotation converged in 5 iterations

\*Bold Values: above threshold value

\*\*Bold elements: elements in the same factor

component matrix (Fig. 4). The component plots in the rotated space denote elements that exist in each stage of factor analysis and in the residual and major elements placed near each other are similar in the fourth and fifth stages. As a result, Cu, Mo and Ag are similar and are paragenesis elements in factor 5–1.

4.2. Application of C–V fractal modeling

Results obtained by SFA revealed that Cu and Mo are situated in a factor as F1–5. Therefore, F1–5 was selected for fractal modeling. The distribution of F1–5 is near to normal with mean value of 0.048. Based on the geometrical properties and grid of the borehole dimensions, the Takht-e-Gonbad deposit was modeled by 10 × 10 × 10 m voxels (David, 1970). F1–5 values were estimated using ordinary kriging (OK) based on the variography parameters, as depicted in Fig. 3. Threshold values of F1–5 were determined in the C–V log–log plot as breakpoints (Fig. 5), which reveals a power-law relationship between F1–5 concentrations and volumes occupied. Breakpoints represent threshold values on the log–log plot. Four breakpoints exist in the C–V log–log plot (Table 3). Supergene enrichment and hypogene zones are

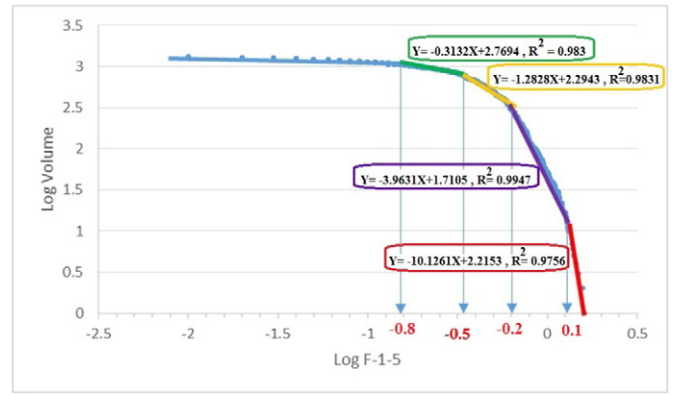


Fig. 5. Log–log plot of volume versus F1–5 values in Takht-e-Gonbad deposit.

considered with F1–5 values >1.26 and 0.63–1.26, respectively. The range for oxidation and leached zones are 0.32–0.63 and 0.16–0.32, based on the C–V fractal modeling.

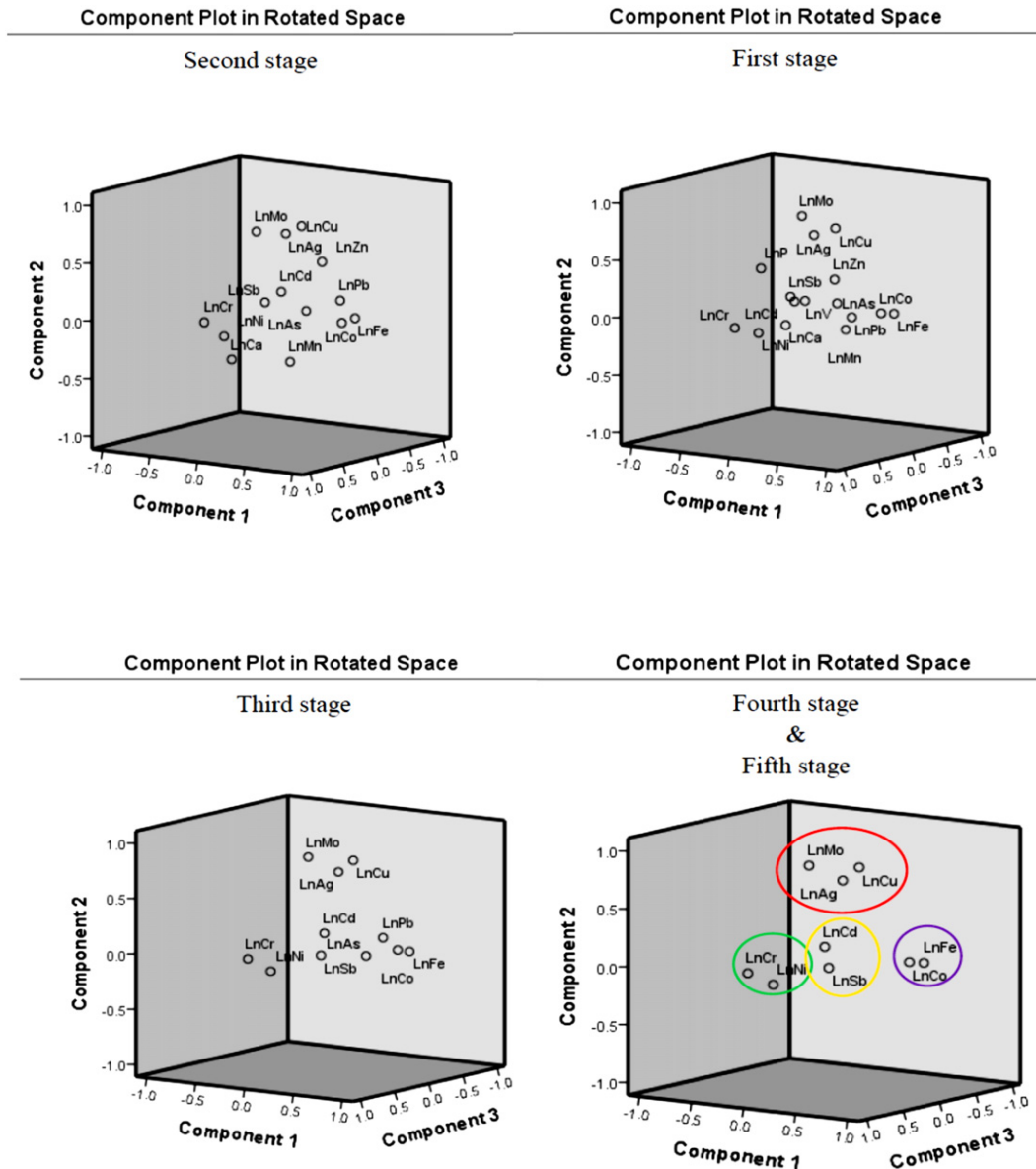


Fig. 4. Component plots in rotated space by five stages of factor analysis.



**Table 3**  
Ranges of F1–5 values for mineralized zones in Takht-e-Gonbad deposit defined from the C–V fractal model.

Zones	Range F1–5
Barren host rock	<0.16
Leached	0.16–0.32
Oxide	0.32–0.63
Hypogene	0.63–1.26
Supergene	>1.26

**5. Correlation between results obtained from C–V fractal modeling, staged factor analysis and geological characteristics**

Results of C–V model were correlated with the 3D geological zonation model of the deposit (Fig. 3). The results generated by the fractal model were controlled by mineralogical investigations, XRD and SEM. Oxide, hypogene and enrichment supergene mineralized zones were characterized by C–V modeling (Fig. 6). Carranza (2011) provided a method for calculation of overlap correlations between two binary

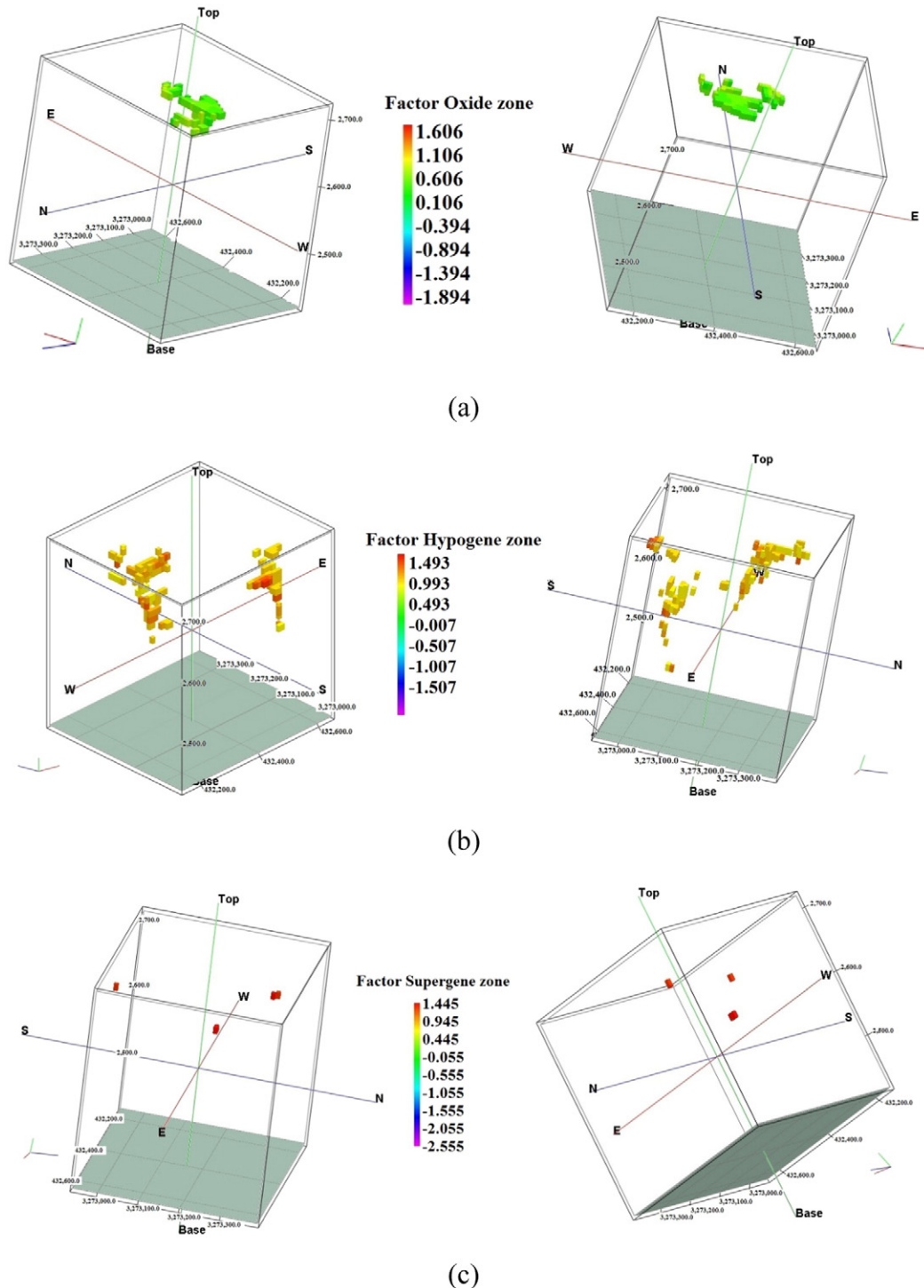


**Fig. 6.** Different mineralized zones based on C–V fractal modeling and staged factor analysis (F1–5) consisting of: a) oxidation b) hypogene and c) supergene enrichment zones.

**Table 4**

Matrix for comparing performance of fractal modeling results with geological model. A, B, C, and D represent numbers of voxels in overlaps between classes in the binary geological model and the binary results of the fractal models (Carranza, 2011).

		Geological model	
		Inside zone	Outside zone
Fractal Model	Inside zone	True positive (A)	False positive (B)
	Outside zone	False negative (C)	True negative (D)
		Type I error C / (A + C)	Type II error B / (B + D)
		Overall accuracy (A + D)/(A + B + C + D)	

models by a logratio matrix. An intersection operation between results of the fractal model and different zones in the geological model was performed to obtain numbers of voxels corresponding to each of the four classes of overlapped zones (Table 4). Type I error (T1E), Type II error (T2E), and overall accuracy (OA) of the fractal model were estimated with respect to the zonation model, based on the fractal and geological block models (Nazarpour et al., 2014).

Correlation between the results obtained by the C–V fractal model and the zonation model derived via geological model show that the supergene enrichment zone has more OA (0.81) compared with the other zones. Additionally, overall accuracies of the oxidation and hypogene mineralized zones are 0.79 and 0.80, respectively, as depicted in Tables 5 to 7.

The means of Cu and Mo values in each resulted supergene enrichment zone identified by log–log plot of F1–5 are 1.16% for Cu and 241 ppm for Mo (Table 8). The hypogene mineralized zone derived via staged factor analysis and C–V fractal modeling has Cu and Mo mean values of 0.65% and 109 ppm (Table 8).

## 6. Conclusions

Results obtained by combination of the C–V fractal modeling and SFA show that the hybrid method is properly utilized for determination of different mineralized zones based on the relationship between the factor values (F1–5 including Cu, Mo and Ag in this scenario) enclosed

**Table 5**

Overall accuracy (OA), Type I and Type II errors (T1E and T2E, respectively), resulted from geological model and oxide zonation mineralized zone obtained through C–V fractal modeling of F1–5 data.

		Geological model (zonation)	
		Inside zone	Outside zone
C–V fractal model of Oxide zone	Inside zone	82 (A)	447 (B)
	Outside zone	3247(C)	14622 (D)
		Type I error 0.975368	Type II error 0.029664
		Overall accuracy 0.799217	

**Table 6**

Overall accuracy (OA), Type I and Type II errors (T1E and T2E, respectively), resulted from geological model and hypogene zonation mineralized zone obtained through C–V fractal modeling of F1–5 data.

		Geological model (zonation)	
		Inside zone	Outside zone
C–V fractal model of Hypogene zone	Inside zone	6 (A)	285 (B)
	Outside zone	3323(C)	14784 (D)
		Type I error 0.998198	Type II error .018913
		Overall accuracy 0.803892	

**Table 7**

Overall accuracy (OA), Type I and Type II errors (T1E and T2E, respectively), resulted from geological model and supergene zonation mineralized zone obtained through C–V fractal modeling of F1–5 data.

		Geological model (zonation)	
		Inside zone	Outside zone
C–V fractal model of Supergene zone	Inside zone	7 (A)	10 (B)
	Outside zone	3322(C)	15059 (D)
		Type I error 0.99789726	Type II error 0.0006636
		Overall accuracy 0.81889335	

**Table 8**

The means of Cu and Mo concentration in each zone identified by log–log plot of F1–5.

Range F1–5	Average of Cu (%)	Average of Mo (ppm)
0.15–0.31	0.38	69
0.31–0.63	0.53	68
0.63–1.25	0.65	109
>1.25	1.16	241

volumes. Moreover, this method is applicable in the Takht-e-Gonbad Cu–Mo porphyry deposit based on multi-elemental data. The supergene enrichment zone contains F1–5  $\geq 1.26$ , Cu  $\geq 1.16\%$  and Mo  $\geq 241$  ppm. Moreover, different mineralized zones can be recognized via the C–V fractal modeling and SFA. The hybrid method utilizes the relationship between the factor values which includes paragenesis ore elemental concentrations and enclosing volumes for example the values of F1–5 in this scenario (Cu, Mo and Ag) associated with various zones, and satisfies power–law relationships. This method can be applicable to results of factor analysis in different multi-elemental porphyry deposits such as Cu–Mo or Cu–Au for which the spatial patterns of concentration values satisfy a multifractal model.

The supergene enrichment, hypogene and oxidation zones delineated via the SFA and C–V fractal model were correlated with geological zonation models due to the application of logratio matrix. Based on the OAs, the overlapping between the results obtained by the SFA and C–V fractal modeling with geological data are higher than 80% which reveals that the hybrid method is proper for outlining of mineralized zones in the porphyry deposits.

## Acknowledgments

The authors wish to thankfully acknowledge Mr. Behbahani, manager of the Takht-e-Gonbad copper Co. and Ms. Kazemi for providing us with the dataset.

## References

- Afzal, P., FadakarAlghalandis, Y., Khakzad, A., Moarefvand, P., RashidnejadOmran, N., 2011. Delineation of mineralization zones in porphyry Cu deposits by fractal concentration–volume modeling. *J. Geochem. Explor.* 108, 220–232.
- Agterberg, F.P., 1995. Multifractal modeling of the sizes and grades of giant and supergiant deposits. *Int. Geol. Rev.* 37, 1–8.
- Alavi, M., 1994. Tectonic of Zagros orogenic belt of Iran: new data and interpretations. *Tectonophysics* 229, 211–238.
- Asadi, S., Moore, F., Zarasvandi, A., 2014. Discriminating productive and barren porphyry copper deposits in the southeastern part of the central Iranian volcano–plutonic belt, Kerman region, Iran: A review. *Earth-Sci. Rev.* 138, 25–46.
- Berger, B.R., Ayuso, R.A., Wynn, J.C., Seal, R.R., 2008. *Preliminary Model of Porphyry Copper Deposits*. USGS, New York.
- Carranza, E.J.M., 2011. Analysis and mapping of geochemical anomalies using logratio-transformed stream sediment data with censored values. *J. Geochem. Explor.* 110, 167–185.
- Cheng, Q., Agterberg, F.P., Ballantyne, S.B., 1994. The separation of geochemical anomalies from background by fractal methods. *J. Geochem. Explor.* 51, 109–130.
- Cox, D., Singer, D., 1986. *Mineral deposits models*. U.S. Geol. Surv. Bull. (1693 pp.).



- Dargahi, S., Arvin, M., Pan, Y., Babaei, A., 2010. Petrogenesis of post-collisional A-type granitoids from the Urumieh Dokhtar magmatic assemblage, Southwestern Kerman, Iran: constraints on the Arabian–Eurasian continental collision. *Lithos* 115, 190–204.
- David, M., 1970. *Geostatistical Ore Reserve Estimation*. Elsevier, Amsterdam (283 pp.).
- Davis, J.C., 2002. *Statistics and Data Analysis in Geology*. 3th ed. John Wiley & Sons Inc., New York (342–353 pp.).
- Fabrigar, L.R., Wegener, D.T., MacCallum, R.C., 1999. Practical assessment research & evaluation. *Costello & Osborne, Exploratory Factor Analysis* 32. vol. 10, No 79.
- Filzmoser, P., Hron, K., Reimann, C., 2009. Principal components analysis for compositional data with outliers. *Environmetrics* 20, 621–632.
- Geological Survey of Iran, 1973. *Exploration for ore deposits in Kerman region*. Rep. Yu/53 (247 pp.).
- Gholami, R., Moradzadeh, A., Yousefi, M., 2012. Assessing the performance of independent component analysis in remote sensing data processing. *J. Indian Soc. Remote Sens.* 40, 577–588.
- Hassanpour, S., Afzal, P., 2013. Application of concentration–number (C–N) multifractal modeling for geochemical anomaly separation in Haftcheshmeh porphyry system, NW Iran. *Arab. J. Geosci.* 6, 957–970.
- Hosseini, M.R., 2012. *Mineralogy, Geochemistry, Fluid Inclusion and Genesis of Takht-e-Gonbad Copper Deposit, Northeast Sirjan* (M.Sc. thesis) Tarbiat Modares University, Tehran, Iran (257 pp. (in Persian with English abstract)).
- Hosseini, M.R., Ghaderi, M., Alirezaei, S., 2011. Geology, alteration and mineralization characteristics of Takht-e-Gonbad copper deposit, northeast Sirjan. *Proceedings of the 1st World Copper Congress, Tehran, Iran*, pp. 160–170 (in Persian with English abstract).
- Kaiser, H.F., 1958. The varimax criteria for analytical rotation in factor analysis. *Psychometrika* 23, 187–200.
- Li, C., Ma, T., Shi, J., 2003. Application of a fractal method relating concentrations and distances for separation of geochemical anomalies from background. *J. Geochem. Explor.* 77, 167–175.
- Lowell, J.D., Guilbert, J.M., 1970. Lateral and vertical alteration –mineralization zoning in porphyry ore deposit. *Econ. Geol.* 65, 373–408.
- Mandelbrot, B.B., 1983. *The Fractal Geometry of Nature*. W. H. Freeman, San Francisco (468 pp.).
- Nazarpour, A., RashidnejadOmran, N., RostamiPaydar, G., Sadeghi, B., Matroudi, F., MehrabiNejad, A., 2014. Application of classical statistics, logratio transformation and multifractal approaches to delineate geochemical anomalies in the Zarshuran gold district, NW Iran. *Chem. Erde-Geochem.* 75 (1), 117–132.
- Pirajno, F., 2009. *Hydrothermal Processes and Mineral Systems*. Springer, The University of Western Australia, Perth.
- Rahmati, A., Afzal, P., Abrishamifar, S.A., Sadeghi, B., 2014. Application of concentration–number and concentration volume fractal models to delineate mineralized zones in Sheytoor iron deposit, Central Iran. *Arab. J. Geosci.* 8, 2953–2965.
- Reimann, C., Filzmoser, P., 2000. Normal and lognormal data distribution in geochemistry: death of a myth. Consequences for the statistical treatment of geochemical and environmental data. *Environ. Geol.* 39, 1001–1014.
- Robb, L., 2005. *Introduction to ore forming processes*. Blackwell, New York, p. 373 pp.
- Sadeghi, B., Madani, N., Carranza, E.J.M., 2015. Combination of geostatistical simulation and fractal modeling for mineral resource classification. *J. Geochem. Explor.* 149, 59–73.
- Sadeghi, B., Moarefvand, P., Afzal, P., Yasrebi, A.B., DaneshvarSaein, L., 2012. Application of fractal models to outline mineralized zones in the Zaghia iron ore deposit, Central Iran. *J. Geochem. Explor.* 122, 9–19.
- Shafiei, B., Haschke, M., Shahabpour, J., 2009. Recycling of orogenic arc crust triggers porphyry Cu mineralization in Kerman Cenozoic arc rocks, southeastern Iran. *Mineral. Deposita* 44, 265–283.
- Taghipour, N., Aftabi, A., Mathur, R., 2008. Geology and Re–Os geochronology of mineralization of the Miduk porphyry copper deposit. *Resour. Geol.* 2, 143–160.
- Treiblmaier, H., Filzmoser, P., 2010. Exploratory factor analysis revisited: how robust methods support the detection of hidden multivariate data structures in IS research. *Inf. Manag.* 47, 197–207.
- Yousefi, M., Carranza, E.J.M., 2015a. Fuzzification of continuous-value spatial evidence for mineral prospectivity mapping. *Comput. Geosci.* 74, 97–109.
- Yousefi, M., Carranza, E.J.M., 2015b. Prediction-area (P-A) plot and C-A fractal analysis to classify and evaluate evidential maps for mineral prospectivity modeling. *Comput. Geosci.* 79, 69–81.
- Yousefi, M., Carranza, E.J.M., 2015c. Geometric average of spatial evidence data layers: a GIS-based multi-criteria decision-making approach to mineral prospectivity mapping. *Comput. Geosci.* 83, 72–79.
- Yousefi, M., Kamkar-Rouhani, A., Carranza, E.J.M., 2012. Geochemical mineralization probability index (GMPI): A new approach to generate enhanced stream sediment geochemical evidential map for increasing probability of success in mineral potential mapping. *J. Geochem. Explor.* 115, 24–35.
- Yousefi, M., Kamkar-Rouhani, A., Carranza, E.J.M., 2014. Application of staged factor analysis and logistic function to create a fuzzy stream sediment geochemical evidence layer for mineral prospectivity mapping. *The Geol. Soc., London* (Online available).
- Zuo, R., Cheng, Q., Xia, Q., 2009. Application of fractal models to characterization of vertical distribution of geochemical element concentration. *J. Geochem. Explor.* 102, 37–43.